

UC Santa Barbara

UC Santa Barbara Previously Published Works

Title

Influence of Extracellular Polymeric Substances on the Long-Term Fate, Dissolution, and Speciation of Copper-Based Nanoparticles

Permalink

<https://escholarship.org/uc/item/9kg9b42w>

Journal

Environmental Science and Technology, 48(21)

ISSN

0013-936X

Authors

Adeleye, Adeyemi S
Conway, Jon R
Perez, Thomas
[et al.](#)

Publication Date

2014-11-04

DOI

10.1021/es5033426

Peer reviewed

Influence of Extracellular Polymeric Substances on the Long-Term Fate, Dissolution, and Speciation of Copper-Based Nanoparticles

Adeyemi S. Adeleye,^{†,§} Jon R. Conway,^{†,§} Thomas Perez,^{‡,§} Paige Rutten,^{‡,§} and Arturo A. Keller^{*,†,§}

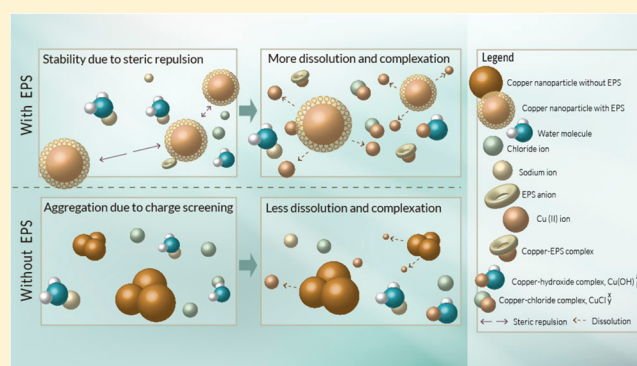
[†]Bren School of Environmental Science & Management, University of California, Santa Barbara, California 93106–5131, United States

[‡]Department of Molecular, Cellular, and Developmental Biology, University of California, Santa Barbara, California 93106–5131, United States

[§]University of California Center for Environmental Implications of Nanotechnology, Santa Barbara, California United States

Supporting Information

ABSTRACT: The influence of phytoplankton-derived soluble extracellular polymeric substances (EPS), pH, and ionic strength (IS) on the dissolution, speciation, and stability of nano-CuO, nano-Cu, and Kocide (a micron sized Cu(OH)₂-based fungicide) was investigated over 90 days. EPS improved the stability of commercial copper-based nanoparticles (CBNPs) in most conditions, in addition to influencing their dissolution. The dissolution rate was pH 4 ≫ pH 7 > pH 11. The presence of EPS correlated with higher dissolved Cu at pH 7 and 11, and lower dissolved Cu at pH 4. More dissolution was observed at higher IS (NaCl) due to complexation with Cl⁻. Dissolution of nano-CuO at pH 7 increased from 0.93% after 90 days (without EPS) to 2.01% (with 5 mg-C EPS/L) at 10 mM IS. Nano-CuO dissolved even more (2.42%) when IS was increased to 100 mM NaCl (with EPS). The ratio of free-Cu²⁺/total dissolved Cu decreased in the presence of EPS, or as pH and/or IS increased. On a Cu mass basis, Kocide had the highest dissolved and suspended Cu at pH 7. However, dissolution of nano-Cu resulted in a higher fraction of free Cu²⁺, which may make nano-Cu more toxic to pelagic organisms.



INTRODUCTION

Global production of copper-based nanoparticles (CBNPs) was estimated at ~200 t/yr in 2010, and is increasing.¹ CBNPs have found use in cosmetics, pigments, paints and coatings, electronics, and pesticides.^{2–4} These applications may lead to direct exposure of CBNPs to the environment due to normal use, product wear-and-tear, and/or end-of-life disposal.¹ Toxicity of CBNPs and composites to organisms has been demonstrated.^{2,5–8} It is therefore important to understand the long-term fate and transformations of these materials in aquatic systems in order to predict exposure to at-risk organisms.

Stability and dissolution of engineered nanoparticles (ENPs) depend on ionic strength (IS), pH, and natural organic material (NOM).^{9–12} Rapid aggregation of nano-Cu was reported in freshwater by Griffith et al.⁵ The authors also found that less than 0.1% of the nano-Cu dissolved in 48 h in the freshwater media used (pH 8.2). 98% dissolution of nano-Cu was however reported at pH 6 in “uterine-fluid” after a week,¹³ demonstrating the importance of pH and media composition on CBNPs’ dissolution. Mudunkotuwa and co-workers¹⁴ reported increased dissolution of aged and new CBNPs in the presence of organic acids. Similarly, Worthington et al.¹⁵ showed that the chitosan improved stability and dissolution of nano-Cu. To our knowledge, no studies have previously

investigated the effects of naturally occurring NOM such as extracellular polymeric substances (EPS) on the stability and dissolution of CBNPs. EPS are synthesized by microorganisms, which are abundant in natural aquatic systems. EPS are mainly composed of polysaccharides, proteins, nucleic acids, and other polymers; and their composition may vary spatially and temporally even within the same species.¹⁶ EPS may interact with ENPs, thus affecting their fate and transformation.¹⁷ Additionally, the long-term fate and transformation of CBNPs in aqueous media has not been reported in the literature.

Studies commonly investigate the aggregation of ENPs in order to predict their environmental fate. In this study, however, we also investigated the fate of a commercial Cu(OH)₂-based product, Kocide 3000 (denoted Kocide). We introduced Kocide, nano-Cu and nano-CuO to a series of aqueous solutions with the goal of investigating the effect of EPS, pH, and IS on (1) stability; and (2) dissolution and speciation over 90 days. To understand the role of EPS, studies

Received: July 10, 2014

Revised: October 3, 2014

Accepted: October 8, 2014

were also conducted in the presence of Suwannee River natural organic matter (SRN).

EXPERIMENTAL SECTION

Copper-Based Nanoparticles. Nano-CuO (Sigma-Aldrich), nano-Cu (U.S. Research Nanomaterials), and Kocide (Dupont) particles were used as received. The size and surface charge were characterized by measuring initial hydrodynamic diameter (HDD) and zeta (ζ) potential (Malvern Zetasizer Nano-ZS90). HDD was an average of 7 measurements with each measurement reflecting 3 runs. Isoelectric point (IEP) was determined by titrating CBNP suspensions with dilute HCl and NaOH. Copper content (wt %) of particles was determined via ICP-AES (iCAP 6300, Thermo Scientific). Further characterizations were done via X-ray diffraction (XRD, Bruker D8 Advance),¹⁸ X-ray photoelectron spectroscopy (XPS, Kratos Axis Ultra), thermogravimetric analysis (Mettler STARe TGA/sDTA851e), Brunau–Emmet–Teller (BET) surface area analysis (Micromeritics TriStar 3000 porosimeter), helium density analysis (Micromeritics AccuPyc II 1340 pycnometer), and scanning electron microscopy (FEI XL30 Sirion equipped with an EDAX APOLLO X probe for energy-dispersive X-ray spectroscopy, EDS).

Stock Suspension Preparation and EPS Characterization. 200 mg/L stock suspensions of CBNPs were bath-sonicated (Branson 2510) for 30 min to disperse the particles. 100 mM buffer stocks (pH 4 = acetate, pH 7 and 11 = phosphate) were prepared and passed through 0.1 μm filter prior to use (final buffer concentration was 0.5 mM for all experiments). A SRN stock solution was prepared as described in Supporting Information (SI). Soluble EPS was extracted from a marine phytoplankton, *Isochrysis galbana*, as described in a previous study¹⁷ and summarized in the SI.

EPS was characterized by measuring carbohydrate and protein concentrations using anthrone method and modified Lowry protein assay, respectively.^{19,20} Total organic carbon (TOC) was determined using a Shimadzu 5000A TOC analyzer. Hydrodynamic diameter of EPS was determined using the Zetasizer. ζ potential of EPS at the conditions of this study and titrimetry were also done using the Zetasizer. Infrared spectroscopy of EPS and SRN was obtained using a Nicolet iS10 FTIR spectrometer with a diamond ATR crystal. Interferograms were obtained by taking 256 scans with a resolution of 2 cm^{-1} .

Aggregation and Sedimentation Kinetics. Aggregation and sedimentation kinetics were studied using the Zetasizer and time-resolved optical absorbency (Shimadzu 1601 UV-vis spectrophotometer) respectively.¹⁷ Detailed information on aggregation, CCC determination and sedimentation experiments are in the SI.

Dissolution, Speciation, And Suspended Cu. Dissolution of each particle was investigated at 10 mg/L in 15 conditions (SI Table S1) at different pH (4, 7, and 11), IS (1, 10, and 100 mM NaCl), and NOM conditions (EPS, SRN, or neither). A pH of 11 is not commonly found in the environment but has been observed in arid soils and the corresponding groundwater and lakes.²¹ Measured aliquots of CBNPs stocks, EPS/SRN/neither, NaCl, and buffer were vortexed to prepare each condition, and transferred directly into Millipore Amicon Ultra-4 10 kDa centrifugal filter tubes (maximum pore size \sim 4 nm), which were kept at 20 °C for increasing time periods (0, 1, 7, 14, 21, 30, 60, and 90 days). To determine dissolution and speciation, the ultrafiltration tubes

were centrifuged for 40 min (Sorvall RC 5B Plus) with a swinging bucket rotor at 4000g. A fraction of the filtrate was analyzed for free cupric ion (f-Cu²⁺) using an ion selective electrode (Cole Parmer). The electrode was calibrated within every hour of use, and lighting was kept constant to minimize the effect of any photoinduced reactions at the electrode probe surface that would cause measurement error. The remaining filtrate fraction was digested and analyzed for total dissolved copper ([Cu]_{diss}) via ICP-AES, as described previously.^{12,22} Complexed cupric ion (c-Cu²⁺) in CuO and Kocide was determined by mass balance: [Cu]_{diss} – f-Cu²⁺. Since nano-Cu may also form some Cu⁺, the mass balance yielded non-f-Cu²⁺ species. Further speciation and complexation of Cu at equilibrium were estimated using Visual MINTEQ 3.0, which was downloaded from <http://vminteq.lwr.kth.se/> and used without modification. CBNPs were input as finite solids based on their copper content and speciation. Kocide was modeled as Cu(OH)₂, nano-Cu was modeled as Cu metal, and nano-CuO was modeled as Tenorite(c). More details about MINTEQ calculations are in the SI.

Additional experiments were set up similar to the dissolution and speciation experiments, but aliquots were not filtered prior to digestion and ICP-AES analyses. In this way, total copper in the supernatant, [Cu]_{total} (dissolved + suspended) could be determined. Suspended copper in the supernatant, [Cu]_{susp} was derived from [Cu]_{total} – [Cu]_{diss}. The pH of suspensions was monitored over time.

RESULTS AND DISCUSSION

Nanoparticle and EPS Characterizations. Major physicochemical properties of CBNPs are presented in Table 1.

Table 1. Physicochemical Properties of Particles Used in This Study

property	nano-CuO	nano-Cu	kocide
primary particle size (nm)	50 ^a	40 ^a	50 × 10 ^{3b}
hydrodynamic diameter ^c (nm)	280 ± 15	2590 ± 1138	1532 ± 580
copper content (wt %)	74.3 ± 1.2	83.3 ± 2.1	26.5 ± 0.9
main copper phase	monoclinic CuO	cubic Cu and Cu ₂ O	orthorhombic Cu(OH) ₂
helium density (g/cm ³)	6.349	6.578	2.399
other elements present	O	C, O	C, O, Na, Al, Si, S, Zn
BET surface area (m ² /g)	12.31 ± 0.05	4.86 ± 0.03	15.71 ± 0.16
isoelectric point (IEP)	6.3	2.1	<3.0
CCC at pH 7 (mM NaCl)	40	ND	ND
estimated water content (wt %) ^d	0.23	0.14	10.84

^aAs provided by the manufacturer. ^bDetermined via electron microscopy. ^cMeasurement was done in DI water at pH 7. ^dEstimated by mass lost at 50–150 °C under nitrogen atmosphere. ND = Nondetect.

Nano-CuO appeared as aggregates of 30–100 nm-size particles, and nano-Cu were nanosized (<100 nm) particles that were mostly aggregated to 500–1000 nm. Kocide particles were 20–200 μm in diameter. SEM images and size distribution histograms of the CBNPs are provided in SI Figures S1 and S2, respectively. Despite its large size, Kocide had the largest

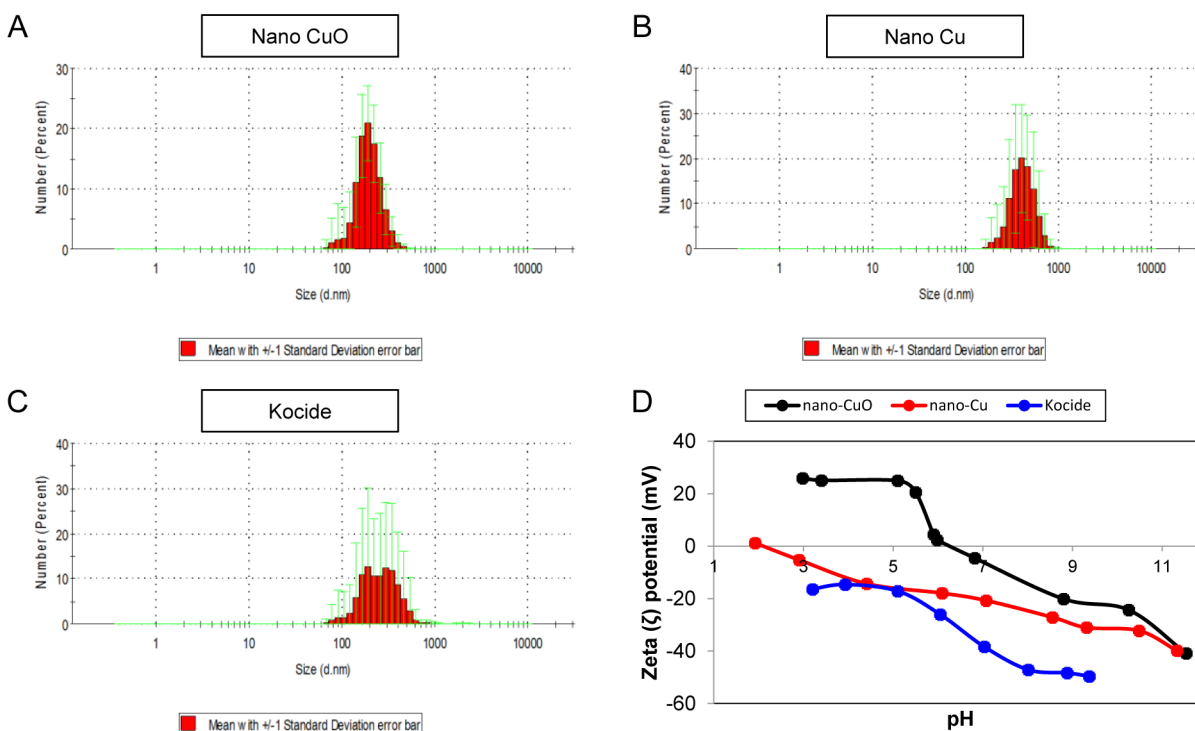


Figure 1. Size distribution of (A) nano-CuO, (B) nano-Cu, and (C) Kocide in DI at pH 7; and surface charge characterization of the three particles across a range of pH, (D).

BET surface area (Table 1) due to surface roughness and porosity. Size distributions of CBNPs in DI at pH 7 are presented in Figure 1. Nanosized particles were detected in the Kocide suspension, suggesting that Kocide particles were broken up in aqueous media. Kocide was negatively charged in the range of pH studied, so its IEP could not be determined. IEP of nano-CuO and nano-Cu was pH 6.3 and 2.1, respectively (Figure 1D). ζ potential of CBNPs in the conditions of this experiment (buffered solution) are shown in SI Table S2. XPS, TGA, and XRD data are shown in SI Figures S3–S5. For TGA, the weight loss in the 50–150 °C temperature range, which corresponds to adsorbed water and surface hydroxyl group was high for Kocide (11%) relative to nano-Cu (0.14%) and nano-CuO (0.23%). In addition, TGA and EDS results (SI Figure S6) suggest high content of carbon (up to 21%) in Kocide, possibly a binder for the particles.

The carbohydrate/protein ratio of *I. galbana*-derived EPS was 3.36. Average HDD and ζ potential of EPS at pH 7 were 204 nm and -24 mV respectively. The net surface charge of EPS and SRN was negative across the range of pH studied (Figure 2A) with SRN being more negative. The FTIR spectra of EPS and SRN are shown in Figure 2B.

Effect of EPS on HDD and Zeta (ζ) Potential. HDD of nano-Cu and Kocide indicated micron-sized particles with broad size distribution as indicated by polydispersity index (PDI) > 0.7 (SI Figure S7). High polydispersity limits the reliability of nanoparticle HDD values,^{23,24} so HDD of nano-Cu and Kocide were not used for further analyses. Nano-CuO was relatively stable in water, with an average HDD of 280 nm. Nano-CuO was however not overly monodisperse, as indicated by a PDI in the range from 0.1 to 0.4.^{23–25} HDD of nano-CuO increased significantly ($t = 2.929$, $p = 0.01$) from 280 to 308 nm in the presence of EPS (SI Figure S7), probably due to EPS coating the particles. There was however no significant change

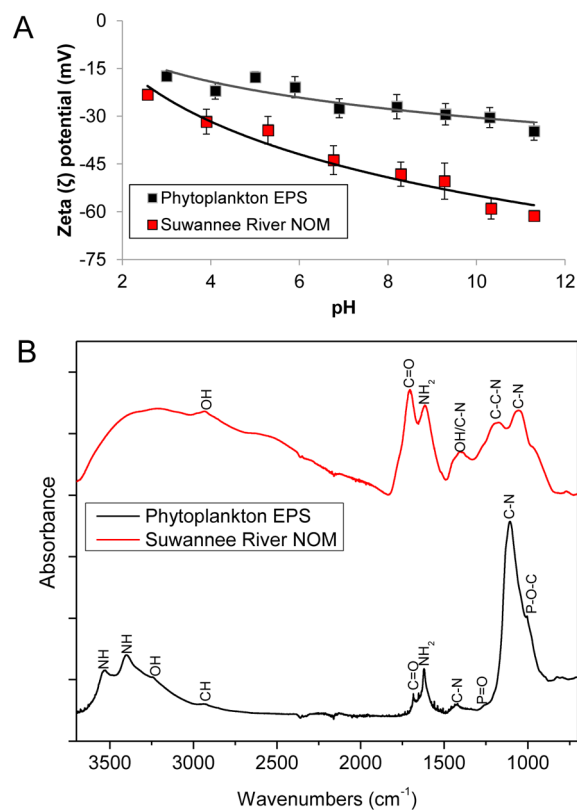


Figure 2. (A) Zeta (ζ) potential (mV) of Suwannee River NOM (SRN) and soluble EPS derived from *Isochrysis galbana* (EPS) as a function of pH. (B) FTIR spectrum of SRN and EPS. Detailed band assignments are provided in SI Table S3.

in size of nano-CuO in the presence of SRN ($t = 0.199$, $p = 0.85$). EDS confirmed the presence of carbon on nano-CuO in

the presence of both EPS and SRN, and the absence of carbon when neither was present.

At pH 7 (buffered solution) ζ potential (in mV) of nano-CuO decreased in magnitude from -34 to -25 in the presence of EPS (ζ potential_{EPS} = -24), and increased in magnitude to -41 in the presence of SRN (ζ potential_{SRN} = -44). ζ potential (mV) of nano-CuO at pH 4 changed from $+43$ in buffered solution to -22 and -26 when EPS and SRN were present, respectively. A similar but weaker trend was observed for nano-Cu and Kocide (Figure 3). Patterns in HDD and ζ potential of

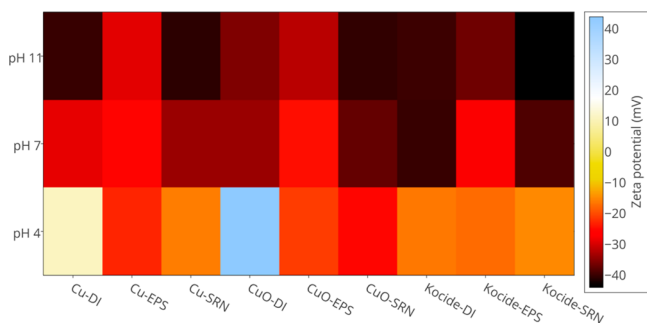


Figure 3. Effect of EPS, SRN, and pH on zeta potential of nano-CuO, nano-Cu, and Kocide. Relative standard deviations (RSD) for zeta potential obtained in the presence of EPS were $\leq 6\%$ except in Kocide where we saw an RSD of 12.5%.

nano-CuO suggest that 5 mg-C/L EPS effectively coated the surface of the particles, which imparted steric stabilization in addition to influencing the surface charge (electrosteric stabilization). To confirm this, measurement of nano-CuO ζ potential at pH 7 in increasing amounts of EPS (0–5 mg-C/L) showed a gradual change from -34 to -25 , which is approximately equal to the ζ potential of EPS. Similar analyses suggest that nano-Cu and Kocide were not completely coated by the amount of EPS used in this study (probably due to their large size in aqueous media) and that SRN mainly imparted electrostatic stabilization at the concentration used (5 mg/L).

Effect of EPS on Aggregation and Sedimentation Kinetics. Aggregation kinetics and CCC were not determined

for nano-Cu and Kocide due to the high polydispersity of the particles. The CCC of nano-CuO was ~ 40 mM NaCl at pH 7 in the absence of NOM (SI Figure S8). CCC increased to ~ 75 mM in the presence of 0.25 mg/L SRN but could not be determined in the presence of EPS due to steric stabilization (which typically does not follow the classical DLVO theory²⁶). Similarly, nano-CuO was relatively stable up to 10 mM at pH 11 in the absence of NOM. Stability decreased at pH 4 as nano-CuO aggregated rapidly at IS ≥ 10 mM (SI Figure S9), probably due to rapid dissolution (Cu^{2+} ions released from dissolving particles may have subtle effects on electrostatic double layer/repulsion). Similarly, particles sedimented faster at pH 4 than pH 7 or 11: We observed 64%, 40%, and 39% sedimentation after 6 h when nano-CuO was suspended in 10 mM NaCl at pH 4, 7, and 11, respectively (SI Figure S9). The HDD at pH 7 was not significantly different from the HDD at pH 4 ($t = 2.139$, $p = 0.05$), and pH 11 ($t = 0.085$, $p = 0.93$) as seen in SI Figure S10.

Among the three particles, Kocide showed the slowest sedimentation (SI Figure S11), probably due to higher surface charge (Figure 3, SI Table S2) and high content of stabilizer. In addition, Kocide also has a relatively low density and very rough surface, both of which may have improved its buoyancy. Normalized absorbance (A/A_0 , where A = absorbance and A_0 = initial absorbance) after 6 h in 10 mM IS at pH 7 was 0.60, 0.25, and 0.74 for nano-CuO, nano-Cu, and Kocide, respectively. Rapid dissolution of nano-Cu at low pH and high IS obscured accurate measurement of sedimentation at those conditions—the dissolution products (mostly pale blue Cu^{2+}) absorb more strongly than the dark-brown nano-Cu particles.

I. galbana EPS decreased aggregation of nano-CuO to a much greater extent than SRN (Figure 4). Decreased aggregate size resulted in decreased sedimentation, especially at high IS. A similar but weaker pattern was observed for Kocide and nano-Cu. Complete sedimentation data for CBNPs are presented in SI Figure S12.

Effect of EPS on Dissolution and Speciation. *Total Dissolved Cu.* In general, dissolution rate was Kocide > nano-Cu \gg nano-CuO. In terms of pH, dissolution was pH 4 \gg pH 7 > pH 11 for the three CBNPs. At pH 4 $[\text{Cu}]_{\text{diss}}$ peaked for

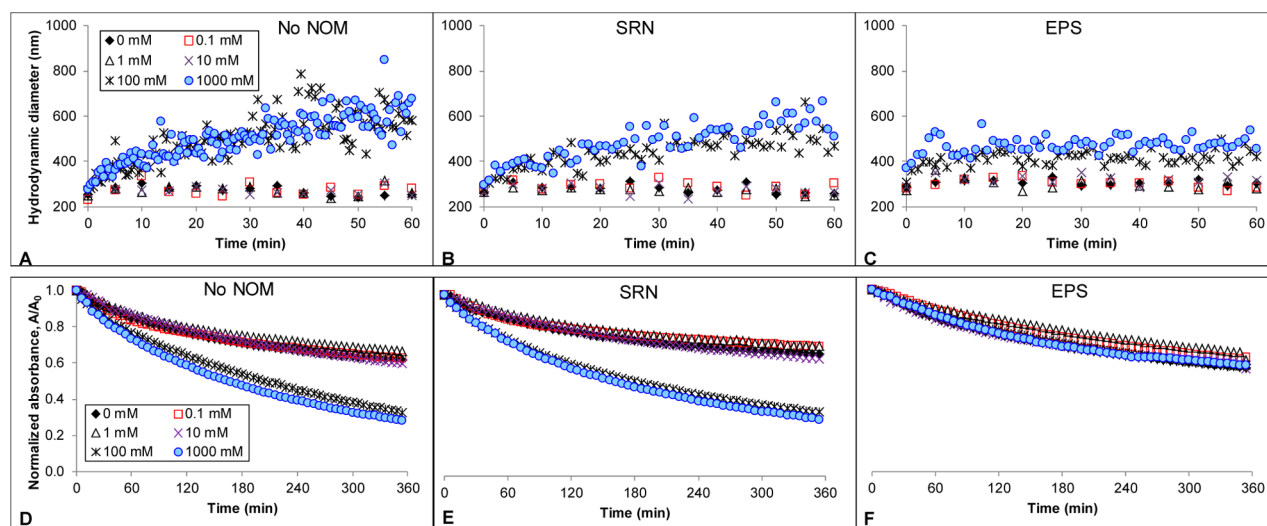


Figure 4. Aggregation kinetics of nano-CuO at pH 7 in (A) absence of NOM, (B) 5 mg/L SRN, (C) 5 mg-C/L EPS, and sedimentation kinetics of nano-CuO in (D) absence of NOM, (E) 5 mg/L SRN, and (F) 5 mg-C/L EPS. Relative standard deviation <math>< 4.5\%</math>.

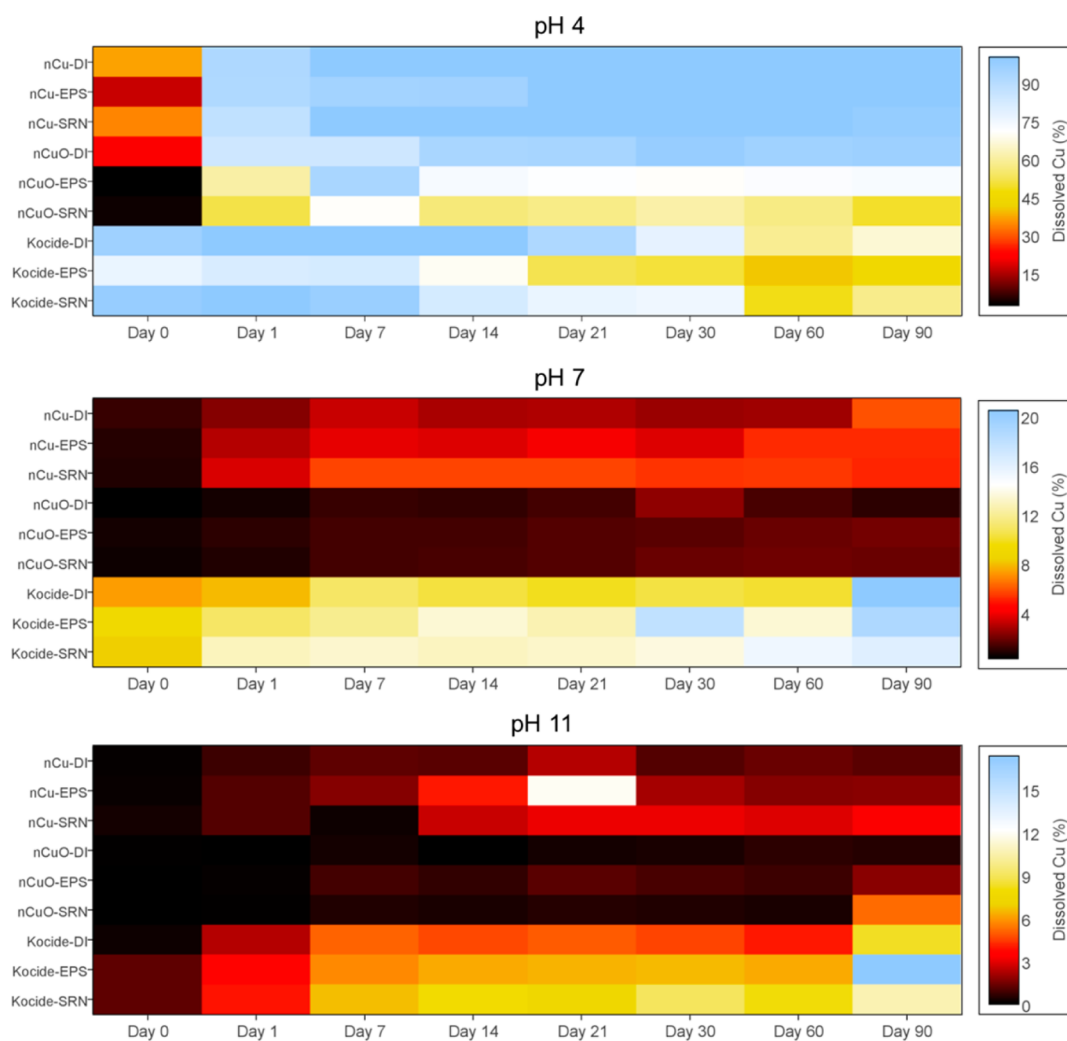


Figure 5. Effect of NOM and pH on 90-day $[\text{Cu}]_{\text{diss}}$ from nano-Cu, nano-CuO, and Kocide. IS = 10 mM NaCl.

Kocide, nano-Cu, and nano-CuO around 2–24 h (100%), Days 1–7 (100%), and Days 21–30 (98%) respectively. Unlike nano-Cu and nano-CuO however, we observed a decreasing $[\text{Cu}]_{\text{diss}}$ in Kocide at pH 4 from Day 21 (Figure 5), probably due to precipitation of Cu-containing species like $\text{Cu}(\text{OH})_2$ and CuO .²⁷ We observed an increase in pH over time in all pH 4 samples (pH 5–6 by Day 90), while pH decreased over time at pH 11 (pH 7–8 by Day 90). There was only a slight decrease in pH at pH 7. Rapid dissolution of Kocide is beneficial for its use as a pesticide but may have important influence on susceptible aquatic organisms if released into natural waters—from excess pesticide application or accidental release.

EPS and SRN slowed down dissolution of CBNPs at pH 4: $[\text{Cu}]_{\text{diss}}$ from nano-CuO decreased from over 21% without NOM after 2 h to about 2.3% and 4.0% in the presence of EPS and SRN respectively (Figure 5). $[\text{Cu}]_{\text{diss}}$ from nano-Cu at pH 4 after 2 h was 34%, 17% and 37% in the presence of SRN, EPS, or neither, but the effect of NOM decreased over time. Similarly, EPS decreased dissolution of Kocide from 96% to 77% after 2 h at pH 4, but SRN did not have an obvious effect. The weaker effect of EPS on dissolution of nano-Cu and Kocide may be due to the large size of these particles, which may result in incomplete coating by EPS. Decreased $[\text{Cu}]_{\text{diss}}$ in the presence of EPS and SRN may have been caused by (1)

steric exclusion of water from the surface of the particles by NOM aggregates, (2) reduced availability of H^+ which may bind to NOM molecules, and/or (3) adsorption of dissolved Cu by NOM aggregates. NOM tend to be protonated and insoluble at low pH,²⁸ and their adsorption onto the CBNPs surface may exclude water to some degree. Due to NOM's insolubility at low pH, they have been shown to sorb more metal ions in acidic conditions, while sorbing less metal ions at basic conditions because they form soluble metal–NOM complexes.²⁹ Protonation of NOM at acidic pH will also reduce the amount of H^+ available to drive dissolution.

$[\text{Cu}]_{\text{diss}}$ from nano-CuO at pH 4 peaked around Days 21–30 in the absence of NOM, but in the presence of EPS and SRN the highest $[\text{Cu}]_{\text{diss}}$ were detected on Day 7. $[\text{Cu}]_{\text{diss}}$ then decreased by about 20% and 14% by Day 14 in the presence of EPS and SRN respectively, and stabilized. The decrease in $[\text{Cu}]_{\text{diss}}$ after reaching the peak concentration was probably due to binding of Cu ions to the functional groups of EPS and SRN. Carboxyl and phosphate groups present in EPS participate in sorption of Cu^{2+} .³⁰ Binding of Cu ions to NOM must have occurred fast (much less than 7 days) but we did not observe it until we sampled on Day 14. Decrease in $[\text{Cu}]_{\text{diss}}$ was also observed for Kocide with and without NOM, but the rate and magnitude of decrease were greater in the presence of EPS and SRN.

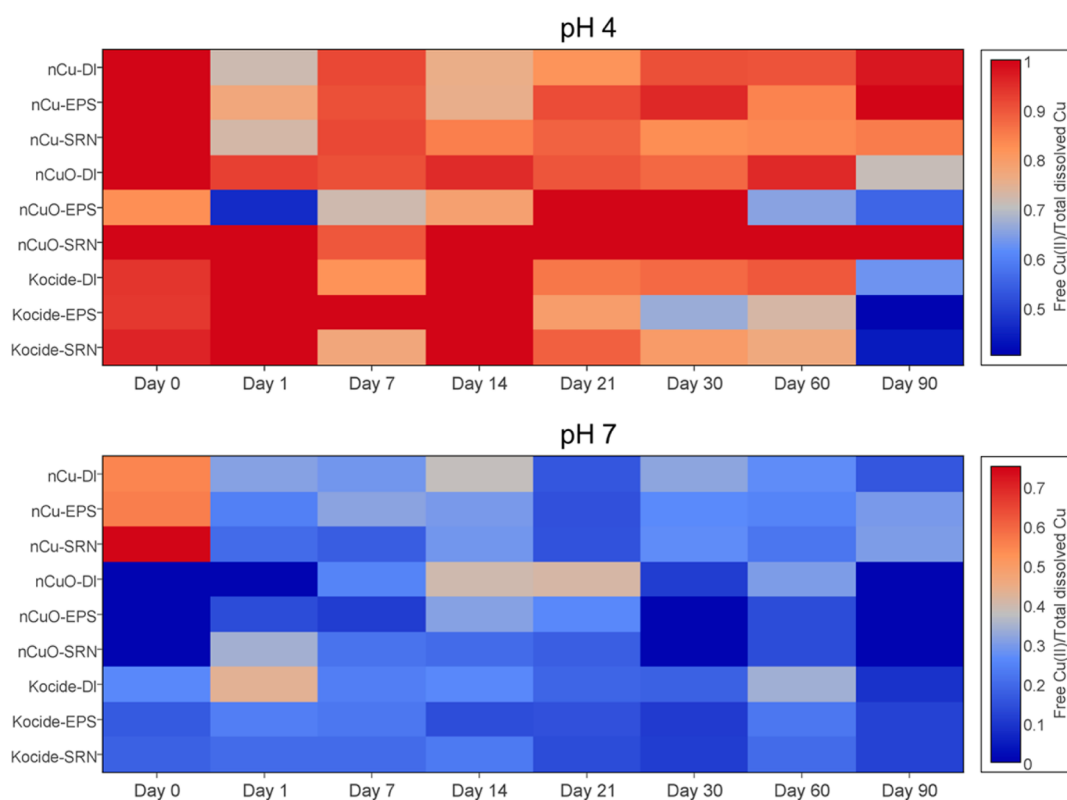


Figure 6. Ratio of Free Cu^{2+} relative to total dissolved Cu at pH 4 and 7. Ratio = 0 for all CBNPs at pH 11 (data not shown).

In contrast to the results seen at pH 4, the presence of EPS and SRN correlated with increased $[\text{Cu}]_{\text{diss}}$ at pH 7 and 11 in all CBNPs (Figure 5). This observation may be adduced to improved stability, solubility of NOM–Cu complexes, and the strength of interactions between NOM and CBNPs. Higher ζ potential obtained at higher pH in the presence of NOM (Figure 3) typically correlated with slower aggregation (see SI Figure S13). Smaller aggregate sizes at pH 7 and 11 (relative to pH 4) may thus have contributed to enhanced dissolution. Unlike at acidic conditions where NOM (and thus associated Cu species) may be insoluble, NOM typically forms soluble metal complexes at neutral and alkaline pH conditions. As such we detected the dissolved Cu associated with NOM at pH 7 and 11, but not at pH 4. Increased dissolution may also be explained by the strength of interactions between NOM and particles: Figure 2A and SI Table S2 suggest that electrostatic interactions between NOM and CBNPs will be least at pH 11 and highest at pH 4. This implies that binding of NOM to CBNPs, and thus steric exclusion of water, is not as strong at pH 7 and 11 compared to pH 4.

Dissolution of CBNPs increased with IS under most conditions (SI Figure S14) due to formation of soluble Cl^- complexes; more so in the presence of NOM. For instance, average dissolution of Kocide at pH 7 over 90 days increased from 7.0%, 10.9%, and 17.4% at 1, 10, and 100 mM respectively to 12.7%, 13.5%, and 20.7% in the presence of EPS; and 8.4%, 13.2, and 18.8% in the presence of SRN. These results imply that rapid sedimentation of CBNPs in natural waters with high IS may not necessarily decrease the exposure to pelagic organisms, as NOM may increase the release of Cu ions, but probably in complexed forms. Additional information on effect of pH and IS on dissolution is in the SI (sections S5.0 and S6.0).

Speciation. The ratio of free Cu^{2+} to total dissolved Cu, $f\text{-Cu}^{2+} / [\text{Cu}]_{\text{diss}}$, was determined in order to understand how different solution chemistries may influence speciation of dissolved Cu. $f\text{-Cu}^{2+}$ species are more bioavailable,³¹ hence, $[\text{Cu}]_{\text{diss}}$ and $f\text{-Cu}^{2+}$ levels may be useful for predicting the availability and toxicity of CBNPs in natural waters. A prediction of pH-dependent speciation obtained using MINTEQA2 is shown in SI Figure S15, and the trend in $f\text{-Cu}^{2+}$ agreed well with experimental findings. Experimentally, $f\text{-Cu}^{2+} / [\text{Cu}]_{\text{diss}}$ decreased in the presence of NOM, and with increasing pH and IS (Figure 6, SI Figure S16). At pH 7 $f\text{-Cu}^{2+}$ accounted for 0–55% of $[\text{Cu}]_{\text{diss}}$ detected in CBNPs over 90 days. At pH 4, $f\text{-Cu}^{2+}$ varied with time from 60 to 100%. The lowest concentration of $f\text{-Cu}^{2+}$ in the Kocide/NaCl/ H_2O system at pH 4 was 1.10 mg/L (observed on Day 90) but still accounted for 63% of the $[\text{Cu}]_{\text{diss}}$ detected. Although nano-Cu was expected to release Cu^+ ,^{14,32} we found that $f\text{-Cu}^{2+}$ accounted for $\geq 72\%$ of $[\text{Cu}]_{\text{diss}}$ during the 90 days at pH 4. Cu^+ may oxidize or disproportionate to form Cu^{2+} ions. The most prominent forms of $c\text{-Cu}^+$ and $c\text{-Cu}^{2+}$ predicted by MINTEQA2 at pH 4 are CuCl_2^- and CuCl^+ , respectively. In contrast to pH 4 and 7, $f\text{-Cu}^{2+}$ was nondetect at pH 11 both via direct measurements and modeling. Hydrolysis of Cu^{2+} occurs at alkaline pH so it exists mostly as $\text{Cu}(\text{OH})_4^{2-}$, $\text{Cu}(\text{OH})^+$, $\text{Cu}(\text{OH})_2$, and $\text{Cu}(\text{OH})_3^-$. In general, Kocide had higher amounts of dissolved and suspended Cu than nano-Cu and nano-CuO at pH 7 on Cu mass basis. Nano-Cu, however, had the highest fraction of $f\text{-Cu}^{2+}$. On the basis of this, we predict that exposure to pelagic organisms of these three particles will be nano-Cu \geq Kocide \gg nano-CuO.

The ratio $f\text{-Cu}^{2+} / [\text{Cu}]_{\text{diss}}$ differed based on the presence and type of NOM (Figure 6). For instance, at pH 4 the amount of $f\text{-Cu}^{2+}$ and $[\text{Cu}]_{\text{diss}}$ from nano-CuO decreased in the presence of

EPS and SRN. However, while $f\text{-Cu}^{2+}$ accounted for most of $[\text{Cu}]_{\text{diss}}$ in the presence of SRN, significant amounts of $c\text{-Cu}^{2+}$ were observed in the presence of EPS suggesting that EPS may be a better Cu-complexing agent than SRN at acidic conditions. A similar observation was made in nano-Cu systems at the same pH, as $f\text{-Cu}^{2+}/[\text{Cu}]_{\text{diss}}$ increased in the presence of SRN compared to EPS. Differences in $f\text{-Cu}^{2+}/[\text{Cu}]_{\text{diss}}$ between EPS and SRN at acidic pH may be due to differences in competitive sorption affinity of $f\text{-Cu}^{2+}$ and H^+ for NOM binding sites.³³ Higher complexation of Cu^{2+} by EPS at pH 4 was confirmed by measuring $f\text{-Cu}^{2+}$ in CuCl_2 solution over time in the presence of EPS, SRN, or neither (data not shown).

Complexing agents in the conditions of this study were mainly Cl^- , OH^- , and NOM, and results obtained at pH 7 suggest that dissolution of CBNPs was driven by both $[\text{H}^+]$ and the formation of complexes. Some complexing could occur from buffer components but this is not expected to be significant due to low concentrations of buffer used (0.5 mM). In nano-Cu, for instance, the total amount of $f\text{-Cu}^{2+}$ increased slightly within the first 24 h but in that same period $f\text{-Cu}^{2+}/[\text{Cu}]_{\text{diss}}$ decreased from 1.28 to 0.32 (−75%), 3.06 to 0.26 (−92%), and 1.20 to 0.46 (−62%) in the presence of EPS, SRN, and neither, respectively. As such, NOM appears to contribute somewhat to complexation, but Cl^- and OH^- were the primary complexing agents. Inorganic dissolved Cu in natural waters exists mostly as complexes of carbonate (e.g., CuCO_3 and $\text{Cu}(\text{CO}_3)_2^{2-}$), hydroxide (e.g., $\text{Cu}(\text{OH})_2$, $\text{Cu}(\text{OH})^+$, and $\text{Cu}_2(\text{OH})_2^{2+}$), and NOM.¹¹ The predominant species is highly dependent on the concentrations of OH^- and CO_3^{2-} (i.e., pH and water hardness).¹¹ As we showed in this study, organic ligands from biota in aquatic systems may play an important role in Cu-complexation, and thus, its bioavailability and toxicity to organisms.³⁴

Suspended and Total Cu in Supernatant. The total amount of copper in the supernatant, $[\text{Cu}]_{\text{total}}$, represents the level of Cu to which pelagic organisms are exposed; and it is composed of dissolved ($[\text{Cu}]_{\text{diss}}$) and suspended species ($[\text{Cu}]_{\text{susp}}$). $[\text{Cu}]_{\text{susp}}$ may include suspended undissolved CBNPs and recrystallized particles, as well as Cu ions adsorbed to suspended particles. In general, $[\text{Cu}]_{\text{susp}}$ was highest on Day 0 at all pH conditions, then decreased by about 1–2 orders of magnitude within a day due to sedimentation and dissolution (SI Figure S17). $[\text{Cu}]_{\text{total}}$ decreased rapidly at pH 7 and 11 due to sedimentation and slow dissolution, but generally increased at pH 4 due to rapid dissolution. $[\text{Cu}]_{\text{total}}$ decreased faster at lower IS since there was more dissolution at high IS (SI Figure S18).

$[\text{Cu}]_{\text{susp}}$ was higher in the presence of EPS and SRN in all CBNPs at pH 7 and in most conditions at pH 4 and 11. For example, after a week of dissolution and settling, $[\text{Cu}]_{\text{susp}}$ in nano-CuO system (pH 7, 10 mM) was 0.48, 0.32, and 0.10 mg/L in the presence of EPS, SRN, and neither, respectively. The trend was similar in nano-Cu and Kocide (SI Figure S19). Increased $[\text{Cu}]_{\text{susp}}$ in the presence of NOMs resulted mainly from improved stability of undissolved particles, and binding of Cu ions to suspended particles—including NOMs (mostly at acidic pH) and undissolved/precipitated particles. MINTEQA2 was unable to model Cu ions adsorbed to EPS and SRN separately but estimated Cu^{2+} bound to DOC as 0.8 mg/L at pH 4 in the nano-CuO system. Experimentally for nano-CuO we detected average $[\text{Cu}]_{\text{susp}}$ of 1.59, 2.36, and 0.28 mg/L in the presence of EPS, SRN, and neither, respectively, between Day 30 and 90 at pH 4. At the same pH and time in nano-Cu

system, $[\text{Cu}]_{\text{susp}}$ was 0.36, 0.17, and 0.14 mg/L in the presence of EPS, SRN, and neither, respectively. For Kocide, we found 1.21, 1.18, and 1.0 mg/L in the presence of EPS, SRN, and neither, respectively. Increased suspended CBNPs in the presence of EPS may result in additional toxicity to sensitive species (in addition to toxicity from ions).⁷ Effective regulation of CBNPs may therefore require particle-specific toxicological information (e.g., Shi et al.⁷) in addition to widely used data for copper ions and salts. Overall, results suggest that the long-term fate of CBNPs is the sediment phase, where they will persist. Exposure of benthic organism to CBNPs is therefore likely to be chronic.

At pH 7 and 11, $[\text{Cu}]_{\text{total}}$ was higher in the presence of NOM for all CBNPs due to improved stability and dissolution. Average $[\text{Cu}]_{\text{total}}$ (Day 0–90) in nano-Cu system was 1.80, 1.86, and 1.44 mg/L at pH 7 in the presence of EPS, SRN, and neither, respectively. Average $[\text{Cu}]_{\text{total}}$ in nano-CuO was 1.41, 1.28, and 1.02 mg/L in the presence of EPS, SRN, and neither, respectively. In Kocide, we detected the average $[\text{Cu}]_{\text{total}}$ of 1.20, 1.19, and 1.03 mg/L in the presence of EPS, SRN, and neither, respectively. Hence, similar to $[\text{Cu}]_{\text{susp}}$, $[\text{Cu}]_{\text{total}}$ at pH 7 was $\text{EPS} \geq \text{SRN} > \text{neither}$. These results suggest that exposure of pelagic organisms to Cu species, if there is a release into natural waters, may increase at higher organic material content, particularly EPS. The additional Cu may be complexed with NOM (if ionic) or coated with NOM (if particulate), which may influence bioavailability.

■ ASSOCIATED CONTENT

● Supporting Information

Methods; Tables S1–S3 showing experimental conditions, Zeta potentials of CBNPs, and band assignments; Figures S1–S19 showing SEM micrograms, size distributions, XPS spectra, thermogravimetric analysis, X-ray diffractograms, energy-dispersive X-ray spectroscopy, HDD and PDI, attachment efficiency, pH-dependent aggregation dynamics, effects of pH, IS, and NOM, aggregation and sedimentation kinetics, effect of ionic strength, and pH-dependent speciation, speciation of dissolved species, effect of pH, ionic species, EPS and SRN, and additional references. This material is available free of charge via the Internet at <http://pubs.acs.org>.

■ AUTHOR INFORMATION

Corresponding Author

*Phone: (805) 893-7548; e-mail: keller@bren.ucsb.edu.

Notes

The authors declare no competing financial interest.

■ ACKNOWLEDGMENTS

This material is based upon work supported by the NSF and the EPA under Cooperative Agreement No. DBI 0830117. Any opinions, findings, and conclusions or recommendations expressed in this material are those of the authors and do not necessarily reflect the views of NSF or EPA. We thank the MRL Central Facilities, which are supported by the MRSEC Program of the NSF under Award No. DMR 1121053. We also acknowledge the lab assistance of Sahar El-Abbadi.

■ REFERENCES

(1) Keller, A. A.; McFerran, S.; Lazareva, A.; Suh, S. Global life cycle releases of engineered nanomaterials. *J. Nanopart. Res.* **2013**, *15* (6), 1–17.

- (2) Cioffi, N.; Torsi, L.; Ditaranto, N.; Tantillo, G.; Ghibelli, L.; Sabbatini, L.; Blevè-Zacheo, T.; D'Alessio, M.; Zambonin, P. G.; Traversa, E. Copper nanoparticle/polymer composites with antifungal and bacteriostatic properties. *Chem. Mater.* **2005**, *17* (21), 5255–5262.
- (3) Ren, G. G.; Hu, D. W.; Cheng, E. W. C.; Vargas-Reus, M. A.; Reip, P.; Allaker, R. P. Characterisation of copper oxide nanoparticles for antimicrobial applications. *Int. J. Antimicrob. Agents* **2009**, *33* (6), 587–590.
- (4) Wang, X. W.; Xu, X. F.; Choi, S. U. S. Thermal conductivity of nanoparticle-fluid mixture. *J. Thermophys. Heat Transfer* **1999**, *13* (4), 474–480.
- (5) Griffitt, R. J.; Weil, R.; Hyndman, K. A.; Denslow, N. D.; Powers, K.; Taylor, D.; Barber, D. S. Exposure to copper nanoparticles causes gill injury and acute lethality in Zebrafish (*Danio rerio*). *Environ. Sci. Technol.* **2007**, *41* (23), 8178–8186.
- (6) Hanna, S. K.; Miller, R. J.; Zhou, D. X.; Keller, A. A.; Lenihan, H. S. Accumulation and toxicity of metal oxide nanoparticles in a soft-sediment estuarine amphipod. *Aquat. Toxicol.* **2013**, *142*, 441–446.
- (7) Shi, J.; Abid, A. D.; Kennedy, I. M.; Hristova, K. R.; Silk, W. K. To duckweeds (*Landoltia punctata*), nanoparticulate copper oxide is more inhibitory than the soluble copper in the bulk solution. *Environ. Pollut.* **2011**, *159* (5), 1277–1282.
- (8) Tranquada, J.; Sternlieb, B.; Axe, J.; Nakamura, Y.; Uchida, S. Evidence for stripe correlations of spins and holes in copper oxide superconductors. *Nature* **1995**, *375* (6532), 561–563.
- (9) Keller, A. A.; Wang, H.; Zhou, D.; Lenihan, H. S.; Cherr, G.; Cardinale, B. J.; Miller, R.; Ji, Z. Stability and aggregation of metal oxide nanoparticles in natural aqueous matrices. *Environ. Sci. Technol.* **2010**, *44* (6), 1962–1967.
- (10) Bennett, S. W.; Adeleye, A.; Ji, Z.; Keller, A. A. Stability, metal leaching, photoactivity and toxicity in freshwater systems of commercial single wall carbon nanotubes. *Water Res.* **2013**, *47* (12), 4074–4085.
- (11) Flemming, C. A.; Trevors, J. T. Copper toxicity and chemistry in the environment—A review. *Water Air Soil Pollut.* **1989**, *44* (1–2), 143–158.
- (12) Adeleye, A.; Keller, A.; Miller, R.; Lenihan, H. Persistence of commercial nanoscaled zero-valent iron (nZVI) and by-products. *J. Nanopart. Res.* **2013**, *15* (1), 1–18.
- (13) Cai, S.; Xia, X.; Xie, C. Research on Cu²⁺ transformations of Cu and its oxides particles with different sizes in the simulated uterine solution. *Corrosion Sci.* **2005**, *47* (4), 1039–1047.
- (14) Mudunkotuwa, I. A.; Pettibone, J. M.; Grassian, V. H. Environmental implications of nanoparticle aging in the processing and fate of copper-based nanomaterials. *Environ. Sci. Technol.* **2012**, *46* (13), 7001–7010.
- (15) Worthington, K. L.; Adamcakova-Dodd, A.; Wongrakpanich, A.; Mudunkotuwa, I. A.; Mapuskar, K. A.; Joshi, V. B.; Guymon, C. A.; Spitz, D. R.; Grassian, V. H.; Thorne, P. S. Chitosan coating of copper nanoparticles reduces in vitro toxicity and increases inflammation in the lung. *Nanotechnology* **2013**, *24* (39), 395101.
- (16) Flemming, H.-C.; Neu, T. R.; Wozniak, D. J. The EPS matrix: The “house of biofilm cells”. *J. Bacteriol.* **2007**, *189* (22), 7945–7947.
- (17) Adeleye, A. S.; Keller, A. A. Long-term colloidal stability and metal leaching of single wall carbon nanotubes: effect of temperature and extracellular polymeric substances. *Water Res.* **2014**, *49* (0), 236–250.
- (18) Huang, Y.; Yang, J.-K.; Keller, A. A. Removal of arsenic and phosphate from aqueous solution by metal (hydr)-oxide coated sand. *ACS Sust. Chem. Eng.* **2014**, *2* (5), 1128–1138.
- (19) Morris, D. L. Quantitative determination of carbohydrates with dreywoods anthrone reagent. *Science* **1948**, *107* (2775), 254–255.
- (20) Legler, G.; Mullerplatz, C. M.; Mentgeshttkamp, M.; Pflieger, G.; Julich, E. On the chemical basis of the lowry protein determination. *Anal. Biochem.* **1985**, *150* (2), 278–287.
- (21) Grant, W.; Jones, B. Alkaline environments. *Encycl. Microbiol.* **2000**, *1*, 126–133.
- (22) Su, Y.; Adeleye, A. S.; Huang, Y.; Sun, X.; Dai, C.; Zhou, X.; Zhang, Y.; Keller, A. A. Simultaneous removal of cadmium and nitrate in aqueous media by nanoscale zerovalent iron (nZVI) and Au doped nZVI particles. *Water Res.* **2014**, *63* (0), 102–111.
- (23) *Dynamic Light Scattering: Common Terms Defined*; Malvern Instruments Limited: Worcestershire, UK, 2011.
- (24) *Zetasizer Nano Series User Manual*; Malvern Instruments Limited: Worcestershire, UK, 2008.
- (25) Nidhin, M.; Indumathy, R.; Sreeram, K. J.; Nair, B. Synthesis of iron oxide nanoparticles of narrow size distribution on polysaccharide templates. *Bull. Mater. Sci.* **2008**, *31* (1), 93–96.
- (26) Grasso, D.; Subramaniam, K.; Butkus, M.; Strevett, K.; Bergendahl, J. A review of non-DLVO interactions in environmental colloidal systems. *Rev. Environ. Sci. Biotechnol.* **2002**, *1* (1), 17–38.
- (27) Hidmi, L.; Edwards, M. Role of Temperature and pH in Cu(OH)₂ Solubility. *Environ. Sci. Technol.* **1999**, *33* (15), 2607–2610.
- (28) Balnois, E.; Wilkinson, K. J.; Lead, J. R.; Buffle, J. Atomic Force Microscopy of Humic Substances: Effects of pH and Ionic Strength. *Environ. Sci. Technol.* **1999**, *33* (21), 3911–3917.
- (29) Zhao, G.; Li, J.; Ren, X.; Chen, C.; Wang, X. Few-Layered Graphene Oxide Nanosheets As Superior Sorbents for Heavy Metal Ion Pollution Management. *Environ. Sci. Technol.* **2011**, *45* (24), 10454–10462.
- (30) Fang, L.; Wei, X.; Cai, P.; Huang, Q.; Chen, H.; Liang, W.; Rong, X. Role of extracellular polymeric substances in Cu (II) adsorption on *Bacillus subtilis* and *Pseudomonas putida*. *Bioresour. Technol.* **2011**, *102* (2), 1137–1141.
- (31) Sunda, W.; Guillard, R. Relationship between cupric ion activity and toxicity of copper to phytoplankton. *J. Mar. Res.* **1976**, *34* (4), 511–529.
- (32) Cai, S.; Xia, X.; Xie, C. Research on Cu²⁺ transformations of Cu and its oxides particles with different sizes in the simulated uterine solution. *Corros. Sci.* **2005**, *47* (4), 1039–1047.
- (33) Cabaniss, S. E.; Shuman, M. S. Copper binding by dissolved organic matter: I. Suwannee River fulvic acid equilibria. *Geochim. Cosmochim. Acta* **1988**, *52* (1), 185–193.
- (34) Wang, Z.; Huang, S.; Liu, Q. Use of anodic stripping voltammetry in predicting toxicity of copper in river water. *Environ. Toxicol. Chem.* **2002**, *21* (9), 1788–1795.